How to cite: Angew. Chem. Int. Ed. 2024, e202319536
doi.org/10.1002/anie.202319536

Luminescence Hot Paper

Dynamically Modulating the Dissymmetry Factor of Circularly Polarized Organic Ultralong Room-Temperature Phosphorescence from Soft Helical Superstructures

Jiao Liu[+], Jun-Jie Wu[+], Juan Wei[+], Zhi-Jun Huang, Xin-Yu Zhou, Jin-Ying Bao, Ruo-Chen Lan, Yun Ma, Bing-Xiang Li,* Huai Yang, Yan-Qing Lu,* and Qiang Zhao**

Abstract: Achieving circularly polarized organic ultralong room-temperature phosphorescence (CP-OURTP) with a high luminescent dissymmetry factor (g_{lum}) is crucial for diverse optoelectronic applications. In particular, dynamically controlling the dissymmetry factor of CP-OURTP can profoundly advance these applications, but it is still unprecedented. This study introduces an effective strategy to achieve photoirradiation-driven chirality regulation in a bilayered structure film, which consists of a layer of soft helical superstructure incorporated with a light-driven molecular motor and a layer of room-temperature phosphorescent (RTP) polymer. The prepared bilayered film exhibits CP-OURTP with an emission lifetime of 805 ms and a g_{lum} value up to 1.38. Remarkably, the g_{lum} value of the resulting CP-OURTP film can be reversibly controlled between 0.6 and 1.38 over 20 cycles by light irradiation, representing the first example of dynamically controlling the g_{lum} in CP-OURTP.

[*] Dr. J. Liu,[+] J.-J. Wu,[+] Z.-J. Huang, X.-Y. Zhou, Prof. Dr. B.-X. Li, Prof. Dr. Q. Zhao
College of Electronic and Optical Engineering & College of Flexible Electronics (Future Technology), Nanjing University of Posts and Telecommunications, Nanjing, 210023, China
E-mail: bxli@njupt.edu.cn

Dr. J. Wei,[+] Prof. Dr. Y. Ma, Prof. Dr. Q. Zhao
State Key Laboratory for Organic Electronics and Information Displays & Jiangsu Key Laboratory for Biosensors, Institute of Advanced Materials (IAM), Nanjing University of Posts and Telecommunications, Nanjing, 210023, China
E-mail: iamyma@njupt.edu.cn
iamqzhao@njupt.edu.cn

Prof. Dr. Y.-Q. Lu
National Laboratory of Solid-State Microstructures & Collaborative Innovation Center of Advanced Microstructures & College of Engineering and Applied Sciences, Nanjing University, Nanjing, 210093, China
E-mail: yqlu@nju.edu.cn

Dr. J.-Y. Bao, Prof. Dr. H. Yang
Key Laboratory of Polymer Chemistry and Physics of Ministry of Education Peking University
Beijing 100871, P. R. China

Prof. Dr. R.-C. Lan
Institute of Advanced Materials, Jiangxi Normal University, Nanchang 330022, China

[+] These authors contributed equally to this work.

Materials exhibiting circularly polarized luminescence (CPL) play a vital role in various optoelectronic applications due to their unique ability to provide chiral configurations in the excited state.

This capability enables the production of left- or right-handed circularly polarized light, which can be evaluated by the luminescent dissymmetry factor (g_{lum}). The g_{lum} is a crucial parameter to assess the level of CPL and can be characterized by the equation of $g_{lum} = 2(I_L - I_R)/(I_L + I_R)$, where I_L and I_R represent the intensity of left-handed and right-handed CPL, respectively, and ± 2 represents completely left- or right-CPL. In this context, numerous CPL materials with high g_{lum} values have been developed for different applications such as biological imaging,[1] three dimensional displays,[2] and anti-counterfeiting.[3] Recent advancements have expanded the dimensions of optical signals by integrating ultralong room-temperature phosphorescence (CP-OURTP), which is observable even after the excitation source is removed, into CPL through crystal engineering,[4] copolymerization,[5] and host-guest doping approaches.[6] However, a significant limitation of CP-OURTP lies in its fixed dissymmetry factor, making the on-demand regulation of g_{lum} challenging. This difficulty stems from the complex chirality transfer between the chiral unit and the room-temperature phosphorescent (RTP) emission group in CPL. To our knowledge, there have been no reports of CP-OURTP materials capable of on-demand control of g_{lum}, an aspect crucial for further advancements in this field.

Cholesteric liquid crystals (CLCs),[7] known for their unique stimuli-responsive properties, are increasingly recognized as ideal candidates for creating CPL materials.[8] Particularly, the soft helical superstructure (SHS), is obtained by polymerizing CLC, that can selectively reflect circularly polarized light (i.e., photonic band gap, PBG) that matches the handedness of its helix while transmitting light of the opposite handedness.[9] This selectivity is due to the periodic helix of the self-organized superstructure, which enables the chiral amplification effect. Based on this, we have successfully realized CP-OURTP by combining phosphorescent polymer with helical superstructures, achieving a high g_{lum} value of 1.49 recently.[10] It should be noted that tailoring the self-organized behavior of the SHS enables the tuning of the PBG over a broad spectrum, which can directly influence the g_{lum} of CPL emission. Currently, numerous

groups are directing their attention toward CPL materials, which include a chiral liquid crystal layer and luminescent layer to enhance g_{lum}. For instance, Zheng and Zhu et al.[8a,11] designed relatively stable and bright CPL by fabricating a soft helix bilayer device consisting of a perovskite-polymer layer and a CLC layer, achieving a high g_{lum} value up to 1.9, which approaches the theoretical maximum g_{lum} of 2.0. Hu et al.[12] reported the circularly polarized amplified spontaneous emission with a g_{lum} as high as 1.4 by constructing a flexible membrane device with ultraflexibility containing perovskite nanocrystals and CLC layers. Deng et al.[13] constructed a bilayered circularly polarized room-temperature phosphorescence device with g_{lum} up to +1.24/−1.57, comprising an RTP-emitting layer and a chiral fluorescent helical polymer-doped CLC layer. Inspired by these strategies, we propose an efficient approach to dynamically modulate the g_{lum} of CP-OURTP by designing a bilayered structure film consisting of an RTP layer and molecular motor (M1) doped SHS layer. Introducing a M1 into the SHS offers a way to regulate the reflection properties of helical superstructure remotely and precisely.[14] This leads to a reversible wide-shift in PBG, a broad range of reflection colors, and helix inversion.[15] Consequently, this approach can be an effective strategy for dynamically regulating the g_{lum} of CP-OURTP.

Following aforementioned ideas, we have developed a photo-responsive soft helical architecture, which is composed of a RTP polymer (P1),[10] a SHS (made of HNG7156, R811, RM257 and Irg651), and a light-driven M1 (2-((1-(9H-fluoren-9-ylidene)-2-methyl-2,3-dihydro-1H-cyclopenta[a]-naphthalen-5-yl)oxy)ethyl (10R,13R,17R)-10,13-dimethyl-17-((R)-6-methylheptan-2-yl)-2,3,4,7,8,9,10,11,12,13,14,15,16,17-tetradecahydro-1H-cyclopenta[a]phenanthrene-3-carboxylate)[16] (Figure 1). Here, P1 was selected due to its high phosphorescence quantum efficiency (24 %), long RTP lifetime (805 ms), and excellent

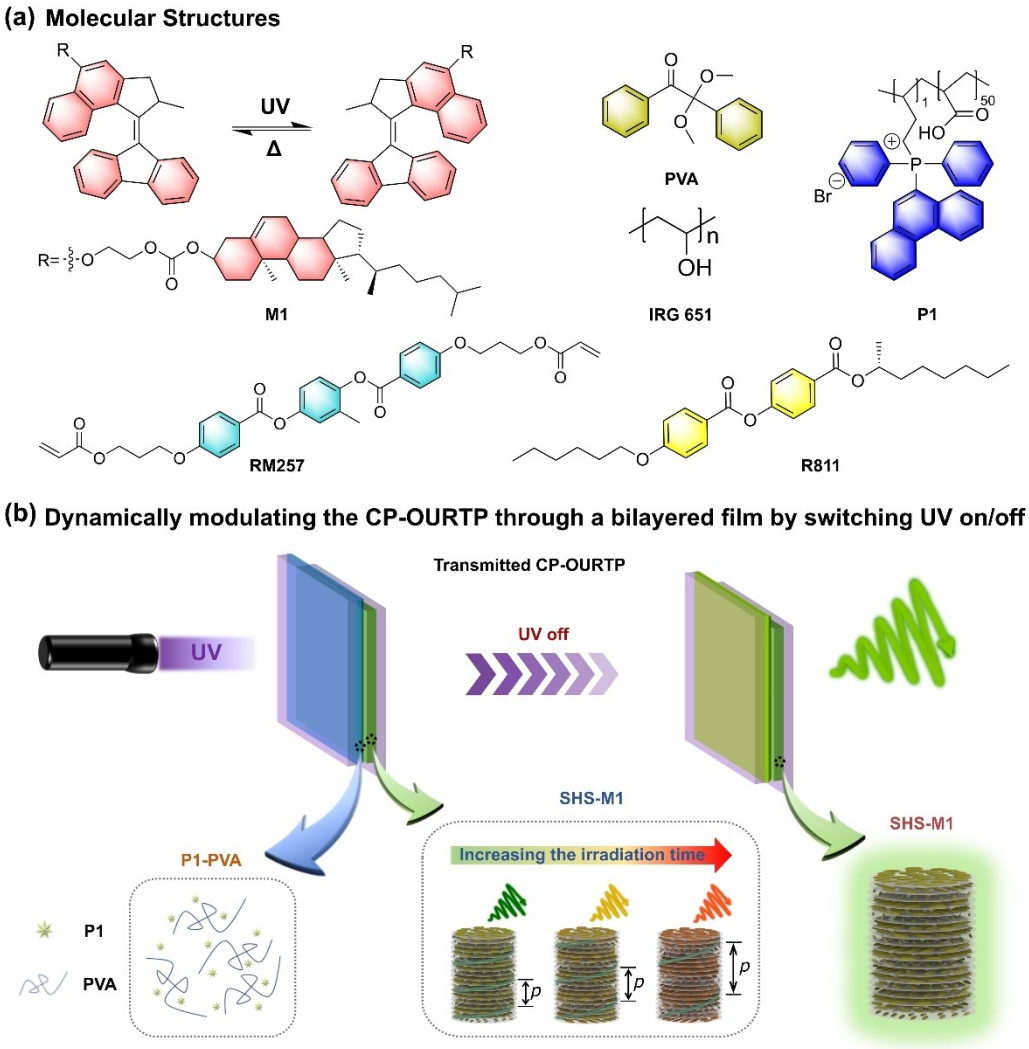

Figure 1. Schematic illustration of dynamically modulating the circularly polarized organic ultralong room-temperature phosphorescence (CP-OURTP). (a) Chemical structures of the material system. (b) Dynamically modulating the CP-OURTP through a bilayered film consisting of soft helical superstructure doped molecular motor (SHS-M1) layer and room-temperature phosphorescent polymer-polyvinyl alcohol (P1-PVA) layer by switching UV light on/off.

processability. The weight average molecular weight (M_w, 38479) and the number average molecular weight (M_n, 36371), synthesis, characterizations, and photoluminescent emission spectra are summarized (Table S1, Figure S1–S6, Supporting Information). SHS was regarded as an ideal medium for enhancing chirality and generating CPL owing to its self-organized helical superstructures. M1 was chosen because it was intricately engineered by incorporating a liquid crystalline cholesterol substituent on the rotor component to enhance the compatibility with liquid crystals. M1 can adopt two interconvertible enantiomers of *M*- and *P*-helical structures that induce the photoinversion of the cholesteric helix upon the exposure to UV light, giving rise to the gradual the successional decrease of g_{lum}.

To achieve the dynamic modulation of PBG and g_{lum} values, a photoresponsive helical liquid crystal system was prepared by fabricating a bilayered P1-SHS-M1 film including SHS-M1 layer by incorporating M1 (5 wt%) into HNG7156, RM257 and Irg651 and doped with different concentration of R811, and a P1-polyvinyl alcohol (P1-PVA) layer (More details in Supporting Information). Figure 2a demonstrates the delayed photoluminescence

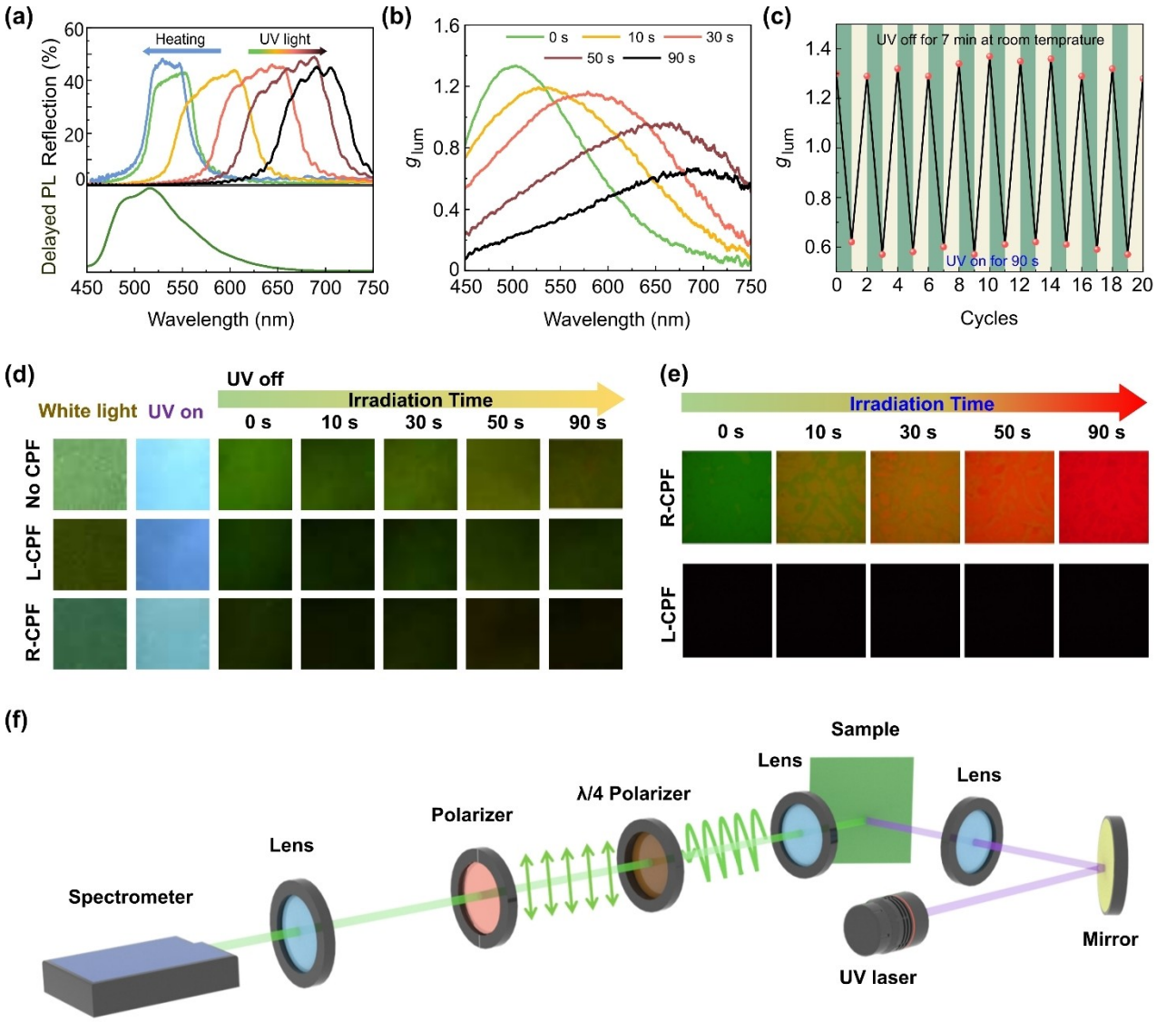

Figure 2. Dynamic modulation of CP-OURTP property in room-temperature phosphorescent polymer-soft helical superstructure-molecular motor (P1-SHS-M1) film when the concentration of R811 is 25.2 wt%. (a) Delayed Photoluminescence (PL) spectra of P1, and the waveband of P1-SHS-M1 was tuned reversibly by altering the irradiation time of 405 nm UV (0 s, 10 s, 30 s, 50 s, and 90 s) and temperature. (b) Luminescent dissymmetry factor (g_{lum}) of P1-SHS-M1 film was dynamically modulated upon different irradiation time of 405 nm UV (0 s, 10 s, 30 s, 50 s, and 90 s). (c) g_{lum} variation during several photoisomerization process and thermal recovery cycles of P1-SHS-M1 film. (d) Photographs of P1-SHS-M1 film taken without a circularly polarized filter (CPF, top), through a left-handed CPF (L-CPF, middle) and a right- handed CPF (R-CPF, bottom) under white light, under 365 nm UV light, and under 405 nm UV for 0 s, 10 s, 30 s, 50 s and 90 s, then irradiated by 365 nm UV for 2 s each time and turn off 365 nm UV. (e) Reflection polarized optical microscopy (POM) images of P1-SHS-M1 under R-CPF and L–CPF upon different exposure time of 405 nm UV. (f) Schematic diagram of circularly polarized luminescence (CPL) measurement.

(PL) spectra (bottom) of P1 and reflection spectra (upper) of P1-SHS-M1 film (the concentration of R811 is 25.2 wt.%) under different irradiation time of 405 nm UV (50 mW cm^{-2}). The emission wavelength of P1 in delayed PL is located at 520 nm. As the increase of the irradiation time (0 s, 10 s, 30 s, 50 s, and 90 s), the reflection band manifests a distinct red shift from 520 nm to 700 nm, along with the reflection color changing from green to red (Figure S7, Supporting Information), which is attributed to the increase of the pitch (p) or the decrease of the helical twisting power (β). p is defined as the distance over which the liquid crystal director rotates around the helical axis by 360°; β represents the capability of the chiral dopant to induce twisting in the nematic liquid crystal.[17] Complete recovery can be achieved by heating the P1-SHS-M1 film at $T=40$ °C for 200 s (Figure S8, Supporting Information). In the CP-OURTP bilayered film, we specifically selected SHS to attain a high g_{lum} at 1.38 by leveraging its characteristic chirality amplification effect. SHS exhibits periodic helical superstructures capable of selectively reflecting circularly polarized light with the same handedness while transmitting the opposite one. The PBG of SHS is intentionally adjusted to overlap with the emission band of P1 by optimizing the concentration of R811 at 25.2 wt.%. Additionally, when exposed to UV light, there is a significant decrease and shift in the g_{lum} values from 1.38 to 0.6 covering the visible range from 500 nm to 700 nm (Figure 2b). In the bilayered film, a right-handed compound (R811) and a right-handed molecular motor (M1) both serve as the chiral dopants. When exposed to UV light, M1 molecules undergo the photoisomerization from a stable state of (*P*)-helicity with right-handedness to an unstable state of (*M*)-helicity with left-handedness, and the transformation process takes approximately 90 s to complete. Durning this photoisomerization, the helical twisting power of M1 drops gradually.[16] The effective p of the bilayered film can be described by the equation (1) below.[18]

$$p = \frac{1}{c_M\beta_M + c_R\beta_R} \quad (1)$$

Where c_M and c_R are the concentrations of M1 and R811, β_M and β_R are the helical twisting power of M1 and R811, respectively. The equation indicates that the overall chirality is determined by these two chiral dopants. As the UV irradiation time increases, β_M decreases, resulting in a gradual increase in the helical pitch. Additionally, due to $|\beta_R| > |\beta_M|$(β_R is approximately 11.7 μm^{-1},[19] β_M will be explained later), and $c_R > c_M$, further increasing UV irradiation time solely contributes to the increase of p, and the chirality inversion is not observed in the bilayered film, as confirmed by Figure S20 (Supporting Information, more details will be discussed further). The central wavelength (λ_c) of PBG is proportional to p when the average refractive index (n) of SHS is constant, based on Bragg's law ($\lambda_c = np$).[20] As a result, λ_c of the reflective band red shifts, which leads to an inadequate overlap of SHS with the emission band of P1. Consequently, g_{lum} gradually decreases[21] with the increase of UV irradiation time, as illustrated in Figure 2b.

The g_{lum} reaches its maximum, approximately 1.38, in the initial state without the irradiation of UV (Figure 2c, indicated by the top red dots). However, with the increase in irradiation time to 90 s, the g_{lum} decreases to a minimum of around 0.6 (Figure 2c, illustrated by the bottom red dots). Subsequently, g_{lum} can return to the initial state after switching off UV light for 7 minutes at room temperature, and this process can be repeated for at least 20 cycles without any fatigue (Figure 2c). As anticipated, in this bilayered film, the handedness inversion of g_{lum} cannot be observed, primarily because of the presence of another chiral dopant, R811, which is present in a higher concentration and has larger β than that of M1. R811 was specifically chosen for doping in SHS due to the compatibility issues between M1 and SHS, when the concentration of M1 exceeds a critical value (22 wt.%) with liquid crystals.[16] Although, M1 can also serve as a chiral agent,[22] the dynamic modulation of g_{lum} in CP-OURTP could not be achieved solely with M1 as the chiral dopant in the visible wavelength range due to its relatively low β and the dispersity issue, even though M1 is specially modified with liquid crystalline cholesterol substituent on the rotor to enhance dispersity with liquid crystals, and the maximum concentration of M1 is up to 22 wt.%.[16] That is, M1 exhibits good dispersity with the liquid crystal at low concentration, as depicted in the polarized optical microscopy (POM) images of Figure 3, but if the concentration of M1 surpasses the critical value, dispersity problems will arise. Therefore, the chiral dopant of R811 in the bilayered film could not be omitted. Based on the characteristic of M1, we are currently capable of dynamically modulating g_{lum} over a wide visible wavelength range by leveraging the combination of R811 and M1, but the handedness inversion of g_{lum} could not be observed in this bilayered film. Similarly, the shift of reflection band can also be observed by altering the intensity of 405 nm UV (Figure S9, Supporting Information). The principle of CPL spectra measurement is demonstrated in Figure 2f. As evidenced by oily-streak textures from POM (Figure S10, Supporting Information), the initial helical arrangements in P1-SHS-M1 are preserved after the irradiation of UV. It could be speculated that UV can availably direct the angular orientation motions of the helical axes triggered by the unique light-responsive dopant of M1, which enables the dynamic reconfiguration switching between planar state and focal conic state, resulting in the dynamic modulation of supramolecular organization and g_{lum} values. P1-SHS-M1 photonic film can be potentially used for optical label (Figure 2d). When a left-handed circularly polarized filter (L-CPF) or a right-handed circularly polarized filter (R-CPF) is used under white light, the label became clearly distinguishable when switching to the R-CPF, signifying P1-SHS-M1 possess right-handed helical axis that can selectively reflect right-handed circularly polarized light but allow the left-handed circularly polarized light to pass through. Upon the irradiation of 405 nm UV, the photonic film can be separated by employing a R- and L-CPF. Subsequently, we first apply 405 nm UV irradiation for 0 s, 10 s, 30 s, 50 s, and 90 s, followed by switching on 365 nm UV (25 mW/cm^2) for 2 s each time. After turning off 365 nm

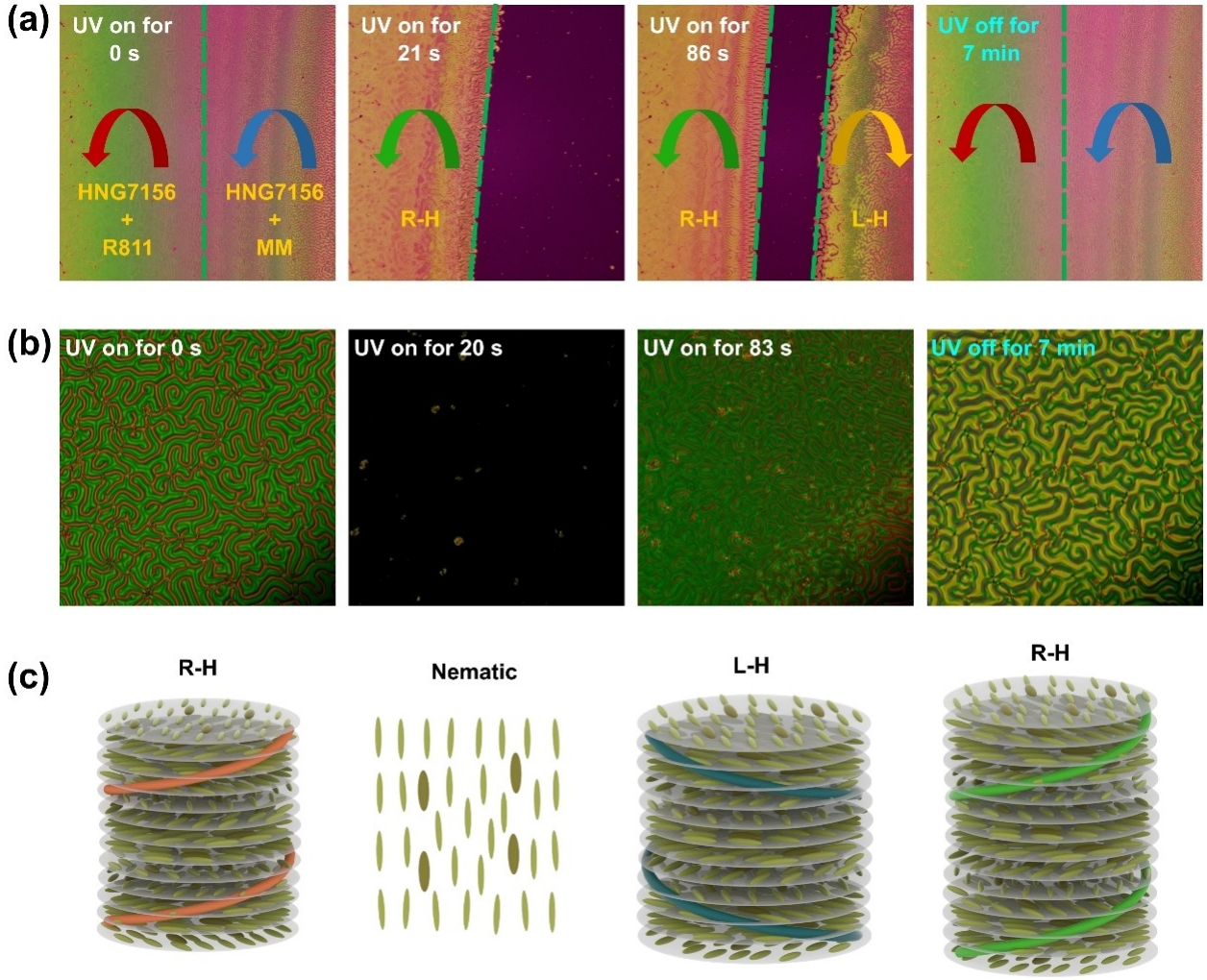

Figure 3. Handedness inversion process of cholesteric liquid crystal (CLC) comprising of HNG7156 and 3 wt% M1. (a) POM images of light driving handedness inversion of the contact preparation sample using a planar alignment cell filled with CLC (right side) and 3 wt% R811 in HNG7156 (left side) upon different irradiation time of UV. (b) POM images of the CLC in a 15.0 μm homeotropic liquid crystal cell under different irradiation time of 405 nm UV. (c) Schematic illustration of light-driven handedness inversion of the CLC, corresponding to Figure 3b.

UV, the afterglow passing through SHS-M1 layer is slightly changed, which is speculated due to the combination of afterglow and dynamic changes of structural color in SHS-M1 induced by the bathochromic shift of the PBG upon the irradiation of 405 nm UV. The POM images in reflection mode under R- or L-CPF with different irradiation time (Figure 2e) were consistent with the reflection bands of Figure S11 (Supporting Information). As expected, similar results were obtained when the concentration of R811 was changed to 20 wt% in P1-SHS-M2 film (Figure S12–S16, Supporting Information). The g_{lum} can also be tuned consecutively under 405 nm UV with different irradiation time, with the typical oily-streak textures maintained (Figure S16, Supporting Information). In this film, the PBG was not matched with the emission peak of RTP at the initial state and the reflection band underwent a narrow shift from 620 nm to 750 nm with the color changing from the earthy yellow to the crimson (Figure S14, Supporting Information). The results indicate that M1 can dynamically adjust the PBG and g_{lum} values upon the irradiation of UV light, which potentially exhibit unique value in the field of encryption application.

To explore the chirality inversion upon the irradiation of UV light, M1 (3 wt%) was doped into a nematic LC host HNG7156, thereby enabling a CLC. p of CLC upon the irradiation of UV light was characterized by the Grandjean-Cano wedge method[23] (Figure S17–S18, Supporting Information). According to the equation $\beta = 1/cp$, p was calculated at 16.06 μm and $\beta = 3.1\ \mu m^{-1}$ in the initial state. Upon the irradiation of 405 nm UV, the distance of the Cano line expanded, thus p increased according to the equation of $p = 2R\tan\theta$, and β was decreased. The Cano line gradually diminished after the irradiation of UV for 60 s (Figure S18, Supporting Information), accompanied by the appearance of a nematic. Further irradiation to 80 s, typical oily-streak textures were observed, implying the occurrence of the handedness inversion of CLC, and the p dropped to 11.02 μm and β increased to $4.53\ \mu m^{-1}$ at the photostationary

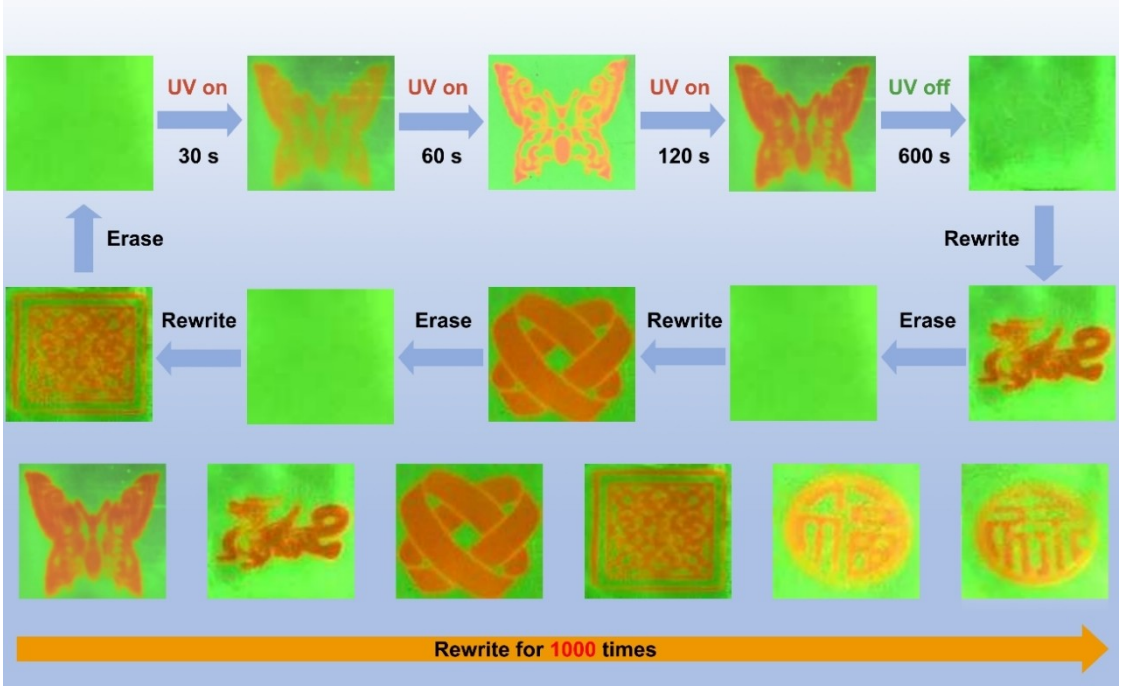

Figure 4. Dynamic and reversible light control of P1-SHS-M1 film upon the irradiation of 405 nm UV by passing through different masks.

state. Subsequently, a nematic emerged after switching off 405 nm UV for 460 s, followed by the formation of the new Cano line after ceasing UV for 1600 s. The whole process suggests that the light driven M1 triggers the handedness inversion of CLC upon the photoisomerization. This inversion is reversible, returning to the initial state upon ceasing the exposure of 405 nm UV light.

Furthermore, we utilized the contact miscibility method to characterize the handedness inversion before and after irradiation of UV (Figure 3). CLC mixture containing HNG7156 and 3 wt.% M1, and a known right-handed CLC comprising of HNG7156 and 3 wt.% R811 were injected into the liquid crystal cell with planar alignment from right side and left side, respectively (Figure S19, Supporting Information). Two samples coalesced immediately after contacting, indicating the mixture of CLC possesses the right handedness (R-H). Upon UV irradiation to 21 s, the CLC on the right side started to disassemble its self-organized helical superstructures until an instantaneous nematic was formed. Further irradiation to 86 s, fingerprint textures emerged, along with an obviously discontinuous boundary (green dashed line) between the new texture and the pre-known right-handed CLC, suggesting the new CLC changed to left handedness (L-H). It is evidenced that the CLC underwent the handedness inversion upon the irradiation of 405 nm UV light and the process can be reversed by ceasing 405 nm UV stimulation. In addition, handedness inversion can also be attained by filling the CLC into a 15.0 μm homeotropic liquid crystal cell through capillary force at 60 °C at its isotropic state, and typical fingerprint textures emerged after cooling down to room temperature (Figure 3b). After exposure to UV for 20 s, the helix fingers disappeared and a nematic occurred. Incessant irradiation to 83 s, new fingerprint textures were observed, signifying that the new formed CLC possess the opposite handedness. After turning off 405 nm UV for 7 min, the CLC can revert to the initial state with the right handedness. The schematic diagram of the handedness inversion is demonstrated in Figure 3c. The whole process provides direct evidence that the CLC underwent the handedness inversion triggered by 405 nm UV in a homeotropic liquid crystal cell. The handedness inversion process in M1 doped HNG7156 was clearly captured by POM images, as depicted in Figure 3, but was not observable in the bilayered film using the Grandjean-Cano wedge method, which is due to the presentence of the chiral dopant of R811 in a high concentration and larger β than that of M1. The pitch of SHS gradually increased with UV irradiation time (Figure S20, Supporting Information), consistent with the result of Figure 2(c). Furthermore, no chirality inversion was detected when M1-doped SHS was injected into a homotropic alignment liquid crystal cell with a thickness of 15 μm (Figure S21, Supporting Information). Overall, chirality inversion could be achieved in M1-doped HNG7156 film but was not detected in the bilayered film. The investigation was then focused on the dynamic handedness inversion of M1 in P1-SHS-M1 film. The P1-SHS-M1 with SHS-M1 side was exposed to 405 nm UV with different irradiation time through butterfly-, dragon-, and paper cutting-patterned masks at room temperature, respectively (Figure S22, Supporting Information). The patterned shapes became more apparent after increasing the irradiation time from 30 s to 60 s, and after exposure to UV light for 120 s, the color of the patterned areas stayed the same, suggesting the complete handedness inversion of M1. It is noteworthy that increasing the temperature enables the erasure of the patterns, along with the maximum wavelength of the

reflection spectra moving from 680 nm to 520 nm (Figure S8, Supporting Information). Based on Bragg's law, the reflectance of P1-SHS-M1 film was strongly associated with the viewing angles (Figure S23, Supporting Information) and exhibited red shift from blue to green by increasing the viewing angles from 30° to 90°. Whereas, upon the irradiation of 405 nm UV for 2 minutes, P1-SHS-M1 showed the blue shift from brownish red to pale yellow as the increase of the viewing angles. Additionally, photo-rewriting of a predefined P1-SHS-M1 can further identify the great advantage of employing M1 (Figure 4). Concretely, a class of meticulously designed patterns written on the photo-responsive liquid crystal using a 405 nm UV as a "pen" by passing through different masks, for example, P1-SHS-M1 film exhibited a well-defined butterfly shape after 405 nm UV irradiation for 120 s, and disappeared after ceasing UV for 600 s. The written information can be entirely self-erased by increasing the temperature to 57 °C. Intriguingly, P1-SHS-M1 film demonstrated the distinguished "write/self-erase/rewrite" ability, which has been substantiated by successive rewriting of butterfly, dragon, topological ring, paper cuttings and Chinese characters "福", "禄". P1-SHS-M1 exhibits multiple switching cycles and can be repeated for over 1000 times without damaging the readability of the patterned information. Simultaneously, the afterglow of P1-PVA film from the other side of P1-SHS-M1 can last for 6 s when irradiated by 365 nm UV (Figure S24, Supporting Information). These multiple advantages, with fast non-invasive light responsive feature, accurate patterning and erasable characteristic enable the optical digital programming.

In summary, we have successfully fabricated a bilayered film with CP-OURTP characteristics by assembling a layer of SHS-M1 liquid crystal and a layer of P1-PVA. The incorporation of the light stimulated M1 enables significant modulation of reflection across a wide spectral range. This modulation varies with different UV light irradiation time and can be reversibly changed by toggling UV light on and off in the P1-SHS-M1 film. As a result, this leads to modulation of the supramolecular organization for the first time, enables the dynamic tuning of the g_{lum} values of CP-OURTP from 1.38 to 0.60. Moreover, the light responsive P1-SHS-M1 film permits precise rewriting of various desired images, patterns, and Chinese characters, which were controlled by UV irradiation and temperature, showing an excellent capability for "write/self-erase/rewrite" cycles. Our approach in dynamically manipulating the g_{lum} values of CP-OURTP paves a new path for controlling multiple dimensions of optical signals and demonstrates promising potential for various advanced optoelectronic applications.

Acknowledgements

The work was supported by the National Key R&D Program of China (2022YFA1405000 and No. 2022YFA1204404), the National Natural Science Foundation of China (No. 62375141), the Natural Science Foundation of Jiangsu Province, Major Project (No. BK20212004), Nanjing University of Posts and Telecommunications Talent Introduction Research Fund Project (Natural Science, No. NY222105), Natural Science Research Start-up Foundation of Recruiting Talents of Nanjing University of Posts and Telecommunications (No. NY222053), and National Natural Science Foundation of China (62322508).

Conflict of Interest

The authors declare no conflict of interest.

Data Availability Statement

The data that support the findings of this study are available in the Supporting Information of this article.

Keywords: Circularly Polarized Luminescence · Room-temperature Phosphorescence · Superstructure · Molecular Motor · Dissymmetry Factor

[1] Y. Sang, J. Han, T. Zhao, P. Duan, M. Liu, *Adv. Mater.* **2020**, *32*, 1900110.
[2] Y. Yang, R. C. da Costa, M. J. Fuchter, A. J. Campbell, *Nat. Photonics* **2013**, *7*, 634.
[3] Y. Shi, J. Han, X. Jin, W. Miao, Y. Zhang, P. Duan, *Adv. Sci.* **2022**, *9*, 2201565.
[4] a) H. Li, J. Gu, Z. Wang, J. Wang, F. He, P. Li, Y. Tao, H. Li, G. Xie, W. Huang, C. Zheng, R. Chen, *Nat. Commun.* **2022**, *13*, 429; b) W. Chen, Z. Tian, Y. Li, Y. Jiang, M. Liu, P. Duan, *Chem. Eur. J.* **2018**, *24*, 17444; c) H. Li, H. Li, W. Wang, Y. Tao, S. Wang, Q. Yang, Y. Jiang, C. Zheng, W. Huang, R. Chen, *Angew. Chem. Int. Ed.* **2020**, *59*, 4756; d) H. Liu, D.-D. Ren, P.-F. Gao, K. Zhang, Y.-P. Wu, H.-R. Fu, L.-F. Ma, *Chem. Sci.* **2022**, *13*, 13922; e) B. Yue, X. Feng, C. Wang, M. Zhang, H. Lin, X. Jia, L. Zhu, *ACS Nano* **2022**, *16*, 16201; f) Y. Gong, L. Zhao, Q. Peng, D. Fan, W. Z. Yuan, Y. Zhang, B. Z. Tang, *Chem. Sci.* **2015**, *6*, 4438.
[5] a) L. Gu, W. Ye, X. Liang, A. Lv, H. Ma, M. Singh, W. Jia, Z. Shen, Y. Guo, Y. Gao, H. Chen, D. Wang, Y. Wu, J. Liu, H. Wang, Y.-X. Zheng, Z. An, W. Huang, Y. Zhao, *J. Am. Chem. Soc.* **2021**, *143*, 18527; b) D. W. Zhang, M. Li, C. F. Chen, *Angew. Chem. Int. Ed.* **2022**, *61*, e202213130.
[6] a) Z. Huang, Z. He, B. Ding, H. Tian, X. Ma, *Nat. Commun.* **2022**, *13*, 7841; b) W. Huang, C. Fu, Z. Liang, K. Zhou, Z. He, *Angew. Chem. Int. Ed.* **2022**, *61*, e202202977.
[7] a) S. Lin, H. Sun, J. Qiao, X. Ding, J. Guo, *Adv. Opt. Mater.* **2020**, *8*, 2000107; b) H. Hu, M. He, X. Liang, M. Li, C. Yuan, B. Liu, X. Liu, Z.-G. Zheng, W.-H. Zhu, *Matter* **2023**, *6*, 3927.
[8] a) S. Liu, X. Liu, Y. Wu, D. Zhang, Y. Wu, H. Tian, Z. Zheng, W.-H. Zhu, *Matter* **2022**, *5*, 2319; b) J. Liu, Z. P. Song, L. Y. Sun, B. X. Li, Y. Q. Lu, Q. Li, *Responsive Materials* **2023**, *1*, e20230005.
[9] B. Liu, C.-L. Yuan, H.-L. Hu, H. Wang, Y.-W. Zhu, P.-Z. Sun, Z.-Y. Li, Z.-G. Zheng, Q. Li, *Nat. Commun.* **2022**, *13*, 2712.
[10] J. Liu, Z. P. Song, J. Wei, J. J. Wu, M. Z. Wang, J. G. Li, Y. Ma, B. X. Li, Y. Q. Lu, Q. Zhao, *Adv. Mater.* **2023**, 2306834. DOI: 10.1002/adma.202306834.
[11] Y. Wu, M. Li, Z.-g. Zheng, Z.-Q. Yu, W.-H. Zhu, *J. Am. Chem. Soc.* **2023**, *145(12951)*, 12951–12966.

[12] W. Lin, C. Yang, Y. Miao, S. Li, L. Zhang, X. F. Jiang, Y. Lv, B. Poudel, K. Wang, L. Polavarapu, C. Zhang, G. Zhou, X. Hu, *Adv. Mater.* **2023**, *35*, 2301573.
[13] X. Wang, B. Zhao, J. Deng, *Adv. Mater.* **2023**, *35*, 2304405.
[14] a) Q. Zhang, D.-H. Qu, H. Tian, B. L. Feringa, *Matter* **2020**, *3*, 355; b) B. L. Feringa, *Adv. Mater.* **2020**, *32*, 1906416.
[15] a) J. Sun, R. Lan, Y. Gao, M. Wang, W. Zhang, L. Wang, L. Zhang, Z. Yang, H. Yang, *Adv. Sci.* **2017**, *5*, 1700613; b) Z. Zheng, H. Hu, Z. Zhang, B. Liu, M. Li, D.-H. Qu, H. Tian, W.-H. Zhu, B. L. Feringa, *Nat. Photonics* **2022**, *16*, 226; c) Y. Li, A. Urbas, Q. Li, *J. Am. Chem. Soc.* **2012**, *134*, 9573–9576.
[16] J. Bao, Z. Wang, C. Shen, R. Huang, C. Song, Z. Li, W. Hu, R. Lan, L. Zhang, H. Yang, *Small Methods* **2022**, *6*, 2200269.
[17] L. Qin, X. Liu, K. He, G. Yu, H. Yuan, M. Xu, F. Li, Y. Yu, *Nat. Commun.* **2021**, *12*, 699.
[18] P. Chen, L.-L. Ma, W. Hu, Z.-X. Shen, H. K. Bisoyi, S.-B. Wu, S.-J. Ge, Q. Li, Y.-Q. Lu, *Nat. Commun.* **2019**, *10*, 2518.
[19] L. Ma, C. Li, L. Sun, Z. Song, Y. Lu, B. Li, *Photonics Res.* **2022**, *10*, 786.
[20] Z. Zheng, H. Hu, Z. Zhang, B. Liu, M. Li, D.-H. Qu, H. Tian, W.-H. Zhu, B. L. Feringa, *Nat. Photonics* **2022**, *16*, 226.
[21] X. Yang, M. Zhou, Y. Wang, P. Duan, *Adv. Mater.* **2020**, *32*, 2000820.
[22] a) W. Kang, Y. Tang, X. Meng, S. Lin, X. Zhang, J. Guo, Q. Li, *Angew. Chem. Int. Ed.* **2023**, *62*, e202311486; b) H. K. Bisoyi, Q. Li, *Chem. Rev.* **2021**, *122(4887)*, 4887–4926.
[23] H. Wang, Y. Tang, H. Krishna Bisoyi, Q. Li, *Angew. Chem. Int. Ed.* **2023**, *62*, e202216600.

Manuscript received: December 18, 2023
Accepted manuscript online: January 24, 2024
Version of record online: ■■, ■■

Research Articles

Luminescence

J. Liu, J.-J. Wu, J. Wei, Z.-J. Huang, X.-Y. Zhou, J.-Y. Bao, R.-C. Lan, Y. Ma,* B.-X. Li,* H. Yang, Y.-Q. Lu,* Q. Zhao* _____ e202319536

Dynamically Modulating the Dissymmetry Factor of Circularly Polarized Organic Ultralong Room-Temperature Phosphorescence from Soft Helical Superstructures

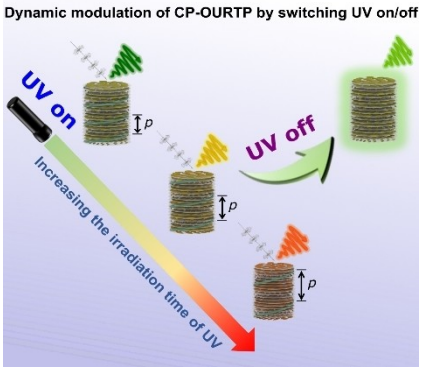

We propose an effective strategy for achieving circularly polarized organic ultralong room-temperature phosphorescence (CP-OURTP) with a high dissymmetry factor based on a bilayered soft helical superstructure doped with a light-driven molecular motor and room-temperature polymer layer. This enables the significant modulation of reflection across a wide spectral range and the dynamic controlling the dissymmetry factor of CP-OURTP from 1.38 to 0.60.